

Internal Structure Optimization of High Power Pulsed IMPATT Diodes

CARLOS CELAYA
Instituto Tecnológico de Puebla
Av. Tecnológico 402, Col. Maravillas
MEXICO

Abstract: - On the basis of the numerical model that includes precise electrical and thermal sub-models, the extremely energy characteristics are investigated of a pulsed-mode Si double-drift IMPATT diodes for 94 and 140 GHz. The optimization of the internal structure of the diode with a traditional doping profile and with complex doping profile is provided. Semiconductor structures with a complex doping profile are analyzed for improving the power level and efficiency of IMPATT diode with a maximum level of permanent current density. The dependencies of power level, efficiency, and admittance have been investigated as functions of feeding current density for the optimum and for near optimum structures. The technological parameter sensitivity analysis is provided for the variation of the total diode length around the optimal value and for the redistribution of the separate parts between the high and the low doping profile level. The complex semiconductor structures may be recommended for the increase of a real time work period and the reliability of the power pulsed-mode diodes.

Key- Words: - Semiconductor microwave devices, modeling and simulation, structure optimization.

1 Introduction

One of the problems of high-power microwave semiconductor electronics is the design and construction of a generator with extraordinary energy characteristics. One of the solutions of this problem is to use pulsed-mode operation. Pulsed-mode IMPATT diodes that are utilized in microwave electronics very frequently have double-drift structures similar to the continuous-mode ones. The idea to use a special form of doping profile for the diode semiconductor structure has been realized in some works [1]-[4]. Modern semiconductor technology provides the possibilities for the fabrication of submicron structures with a complex doping profile. This gives one opportunity to design special IMPATT diode structures for pulsed-mode operation having high feed current values. That is very important for this operation mode because a pulse mode can provide an extreme power value for this type of diode and for all microwave semiconductor devices in general.

The main goal of the present project is analysis of the electrical and thermal processes of pulsed-mode high-power millimetric region IMPATT diode and the internal structure optimization to obtain the maximum output power and energy efficiency. In this work, the extreme energy characteristics of Si double-drift pulsed-mode IMPATT diodes for 94 GHz and for 140 GHz are investigated. The optimization of

the internal structure of the diode with a traditional doping profile, (Fig. 1, curve 1) and with a complex doping profile (Fig. 1, curve 2) is provided.

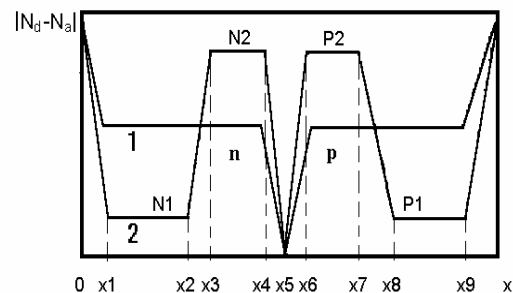


Figure 1. Doping profile for two types of IMPATT diodes:
1 - typical diode structure, 2 - complex diode structure.
x1, x2, ..., x9 are important technological lengths.

We have marked special points of curve 2 on the longitudinal axis for the determination of different technological lengths that are independent parameters of the optimization procedure.

To investigate the physical processes and to optimize the internal diode structure we construct the

new numerical model of the IMPATT diode in section 2 that provide the adequate accuracy and can reduce the total necessary computer time. The optimization procedure more suitable for the microwave device structure optimization is presented in section 3. The main results of the physical analysis and optimization are presented in section 4. The sensitivity of the optimal diode structure's energy characteristics with respect to technological errors is determined too.

2 Problem Formulation

The complex diode model consists of an electrical model that is based on the solution of the continuous equations system (1) jointly with one-dimensional Poisson equation and the thermal model that is based on the solution of heat-conductivity equation (2).

$$\begin{aligned}\frac{\partial n(x,t)}{\partial t} &= \frac{\partial J_n(x,t)}{\partial x} + a_n |J_n(x,t)| + a_p |J_p(x,t)| \\ \frac{\partial p(x,t)}{\partial t} &= -\frac{\partial J_p(x,t)}{\partial x} + a_n |J_n(x,t)| + a_p |J_p(x,t)|\end{aligned}\quad (1)$$

$$\begin{aligned}J_n(x,t) &= n(x,t) V_n + D_n \frac{\partial n(x,t)}{\partial x} \\ J_p(x,t) &= p(x,t) V_p - D_p \frac{\partial p(x,t)}{\partial x}\end{aligned}$$

$$\frac{\partial T}{\partial t'} = \frac{k}{r C} \Delta T + \frac{1}{r C} Q(x, t', T) \quad (2)$$

where Δ is the two-dimensional Laplace operator for the cylindrical coordinate system

$$\Delta T = \frac{\partial^2 T}{\partial x^2} + \frac{1}{r} \frac{\partial}{\partial r} \left(r \frac{\partial T}{\partial r} \right) \quad r \text{ is the radial}$$

coordinate, x is the longitudinal coordinate, T is the Kelvin temperature, r is the material density, C is the specific thermocapacity, k is the thermoconductivity coefficient, and $Q(x, t', T)$ is the internal heat source that, in the general case, has a dependency on the electrical field, current density, and temperature.

Numerical solution of the main system (1) has been obtained by the modification of Crank-Nicolson numerical scheme that is the basis of the work [5], and that has a significant property of absolute stability as demonstrated in [6].

Numerical solution of equation (2) is performed by the iteration method of alternating directions. This model is different from the ones in [7]-[13] because all electrophysical parameters are functions of the electric field and temperature at a corresponding point of the semiconductor structure, and because this model describes the heat source as a function of electric field intensity inside the diode structure. It is very important to take into account the temperature dependency because, just for the pulse mode, there is a high level of permanent and alternative currents, and therefore a high-level variation of temperature in time.

One of the principal characteristics of the optimization procedure is the computer time for one probe of the objective function. Since one probe of the objective function includes the total analysis of the IMPATT diode, it is very important to reduce the complete diode analysis time. The complex diode model of the above mentioned paper [5] is based on the simultaneous use of electronic field and thermal models. This model has great accuracy, but is complicated too, and therefore its functioning is too slow for the optimization problem. On the other hand, other model of the IMPATT diode is used in the present work. This model more suitable just for the optimization problem because this model has computer time for one probe significantly less than in work [5]. This model utilizes the Fourier series analysis [14], and therefore has a limitation, which is inherent in this technique; in particular, this model can be used for stationary process analysis only. However, this model has a great advantage with its shorter computer time, and at the same time, it is a nonlinear model with sufficient accuracy. The other source of computer time reduction is the utilization of the high-order approximation numerical scheme [14] for the thermal equation. These two ideas have been used successfully for the optimization of different types of IMPATT diodes for the different operation modes.

3 Optimization Method

The optimization algorithm was designed as the combination of one of kind of direct method and the gradient method. This is one of the modifications of well-known algorithm, which is successfully used for function with complicate structures. This method is more precisely successful for the optimization of millimetric wave devices because the objective

function of that type of device (for example, the output power) as a function of its arguments has a very complex behavior, similar to a one "valley" in N -dimensional space. The objective function can be determined as the maximum electronic power, for example. The number of free variables for our case is equal to 8. These are four lengths $L1=x2-x1$, $L2=x4-x3$, $L3=x7-x6$, $L4=x9-x8$ and four levels $N1$, $N2$, $P2$, $P1$ of the diode doping profile. We have formed the principal vector of the independent variables $y = \{y_1, y_2, y_3, y_4, y_5, y_6, y_7, y_8\}$ for these eight parameters of the semiconductor structure.

The optimization algorithm consists of the following steps: 1) Given as input two different approximations of two initial points: y^0 and y^1 . 2) At these points, we start with the gradient method, and have performed some steps. As a result, we have two new points Y^0 and Y^1 that are determined by $y^{0n+1} = y^{0n} - \mathbf{d}_n \cdot \nabla F(y^{0n})$, $y^{1n+1} = y^{1n} - \mathbf{d}_n \cdot \nabla F(y^{1n})$, $n = 0, 1, \dots, N-1$, $Y^0 = y^{0N}$, $Y^1 = y^{1N}$, where F is the objective function, \mathbf{d}_n is the parameter of the gradient method. 3) We draw a line through two these points, and perform a large step along this line. We have a new point y^{s+1} : $y^{s+1} = Y^s + \mathbf{a}(Y^s - Y^{s-1})$, $s=1$, where \mathbf{a} is the parameter of the line step. 4) Then we perform a some steps from this point by the gradient method, and obtain a new point Y^s : $y^{s\ n+1} = y^{s\ n} - \mathbf{d}_n \cdot \nabla F(y^{s\ n})$, $s = s+1$, $Y^s = y^{s\ N}$. Then steps 3 and 4 are repeated with the next values of the index s ($s = 2, 3, \dots$).

The optimization process that is presented above cannot find the global minimum of the objective function, but only a local one. To obtain the confidence that we have the better solution of the optimum procedure, it is necessary to investigate N -dimensional space with different initial points. In that case, it is possible to investigate N -dimensional volume in more detail. During the optimization process, it is very important to localize the subspace of the N -dimension optimization space for more detail analysis. The N -dimensional space volume of the independent parameters is determined approximately on the basis of model [14] for the first stage of the optimization procedure. In that case, a Fourier series approximation of principal functions is used, and because of this approximate model, we have a ten times acceleration. After that, on the basis of the precise model [5], we have analyzed the internal structure of two types of silicon diode for 3 and 2 mm region. One of these structures is an

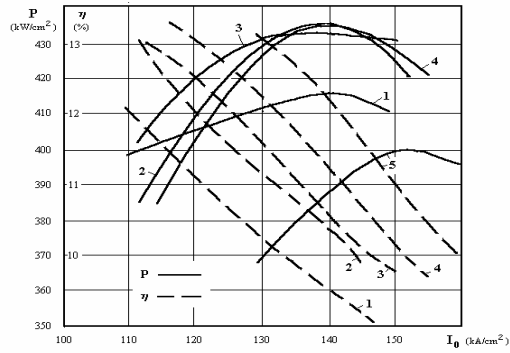
ordinary constant doping profile structure, and the other is a complex one.

4 Results

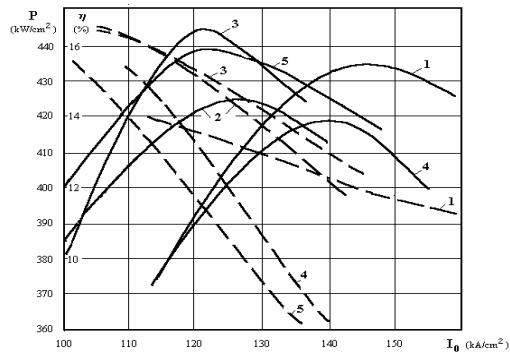
The optimization of the internal diode structure was provided both for the constant doping level and the complex doping level. The aim of the optimization process is not to find the point in the optimization space that provide the maximum value of output power but has a narrow space region. Contrary, we need to find the wide region where the output power has a sufficiently high level but maybe is not a maximum. This solution guarantees better technological implementation. The constant type of doping profile is shown in Fig. 1, curve 1. The complex type of the double-drift IMPATT diode active layer is shown in Fig. 1, curve 2. The width of the p - n junction was given as 0.15 μm and 0.12 μm for 94 GHz and for 140 GHz respectively from the technological aspects. This type of doping profile provides a concentration of electrical field within the p - n junction. The higher level of the ionization rate appears as a result of this doping profile. The electron and hole avalanches have a greater density and a lesser space dimension. On the other hand, for the diode with a constant doping level, the following equalities are corrected: $N1=N2$ and $P1=P2$. In this case, we have only four parameters for the optimization procedure: two lengths $L1=x4-x1$, $L2=x9-x6$ and two doping levels $N1$, $P1$. In this case the optimization process requires less computer time because the smaller dimension of the optimization space.

4.1 94 GHz Diode

In Fig.2 (a), (b) the characteristics of power-level and efficiency for the constant profile diode and complex profile diode for 94 GHz are presented as functions of feeding current density I_0 for the optimum structures and for others that are near the optimum. Parameters of these structures are presented in Table 1 and Table 2. Structure 4 in Fig. 2(a) has the maximum power level 436 kW/cm^2 and the optimal current density value $I_0=140 \text{ kA}/\text{cm}^2$. In that case, the efficiency is equal to 11.2 % for the maximum power point. Structure 5 has a maximum efficiency as the function of the current I_0 , but for the optimum power point this value no larger than for structures 2, 3 and 4. Besides, for this structure it is necessary to increase the current value until 153 kA/cm^2 to obtain of the optimum power point.



(a)



(b)

Figure 2. Output power P and efficiency coefficient μ as functions of the feeding current density I_0 for optimum and near optimum structures for (a) constant and (b) complex doping profile diode.

Table 1. Internal structure parameters for the diode with constant doping profile.

| n | L1 (10^{-4} cm) | L2 (10^{-4} cm) | N1 (10^{17} cm $^{-3}$) | P1 (10^{17} cm $^{-3}$) |
|---|-----------------------|-----------------------|--------------------------------|--------------------------------|
| 1 | 0.35 | 0.33 | 1.5 | 1.5 |
| 2 | 0.35 | 0.33 | 1.65 | 1.68 |
| 3 | 0.35 | 0.33 | 1.7 | 1.7 |
| 4 | 0.35 | 0.33 | 1.9 | 1.9 |
| 5 | 0.35 | 0.33 | 2.1 | 2.1 |

Table 2. Internal structure parameters for the diode with complex doping profile.

| n | L1 | L2 | L3 | L4 | N1 | N2 | P2 | P1 |
|---|-------|-------|-------|-------|------|-----|-----|------|
| 1 | 0.086 | 0.283 | 0.266 | 0.084 | 1.3 | 2 | 2 | 1.3 |
| 2 | 0.065 | 0.212 | 0.203 | 0.063 | 1.3 | 2 | 2 | 1.3 |
| 3 | 0.072 | 0.236 | 0.222 | 0.072 | 1.3 | 2 | 2 | 1.3 |
| 4 | 0.072 | 0.236 | 0.222 | 0.072 | 1.56 | 2.4 | 2.4 | 1.56 |
| 5 | 0.072 | 0.236 | 0.222 | 0.072 | 1.3 | 1.8 | 1.8 | 1.3 |

Semiconductor structures with a complex doping profile are analyzed to improve of the power level and efficiency of pulsed-mode IMPATT diode (Fig. 2 (b)). In that case eight parameters have been varied: $L1$, $L2$, $L3$, $L4$, $N1$, $N2$, $P2$, $P1$. Structure 3 is the optimal one and has an efficiency of about 15% and 446 kW/cm^2 power level at 123 kA/cm^2 . Others structures are near this optimum one but have a lower power level and efficiency. The extension of doping level high parts (structure 1) or increasing this level (structure 4) results to moving the power curve to the greater current density.

Comparison of the optimal characteristics for two different types of the structures as the constant doping profile (curve 4, Fig. 2a) and complex doping profile (curve 3, Fig. 2b) shows that the maximum output power level is quasi equal for two these optimal structures (436 kW/cm^2 and 446 kW/cm^2), but efficiency coefficient has more difference (11.2% and 14.4%). The most important fact is a significant decrease of optimal value of permanent current density for the complex doping structure. The optimal current density value is equal to 140 kA/cm^2 for the constant doping structure, but for the complex doping structure is equal to 123 kA/cm^2 . Therefore the complex doping profile structure has better energy characteristics.

4.2 140 GHz Diode

In Fig.3 (a), (b) the characteristics of power-level, efficiency, and the real and imaginary parts of the complex admittance of the 140 GHz diode are presented as functions of the feeding current density I_0 for the optimum structures and for others that are near the optimum. Parameters of the constant doping level and length values for this figure are presented in Table 3. Structure 4 has a maximum power level of 430 kW/cm^2 and an optimal current density value of $I_0 = 285 \text{ kA/cm}^2$. In that case, the efficiency is equal to 8.0 % for the maximum power point. Structure 5 has a maximum of the negative real admittance and efficiency (8.5 %) but has a smaller power level

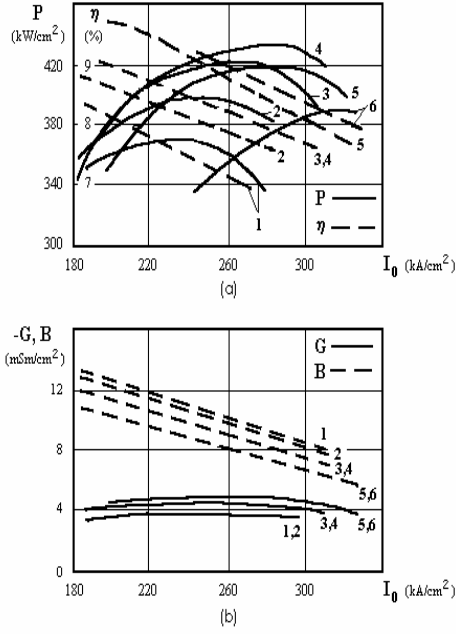


Figure 3. (a) Output power P and efficiency coefficient μ , (b) real G and imagine B parts of the total admittance as functions of feeding current density I_0 for optimal and near optimal structures with constant doping profile level.

Table 3. Internal structure parameters for the diode with constant doping profile.

| n | $L1$ (10^{-4} cm) | $L2$ (10^{-4} cm) | $N1$ (10^{17} cm^{-3}) | $P1$ (10^{17} cm^{-3}) |
|-----|----------------------------------|----------------------------------|---------------------------------------|---------------------------------------|
| 1 | 0.22 | 0.19 | 3 | 3 |
| 2 | 0.24 | 0.19 | 3.5 | 3.5 |
| 3 | 0.21 | 0.19 | 3.5 | 4.5 |
| 4 | 0.21 | 0.19 | 4 | 4 |
| 5 | 0.21 | 0.19 | 4.5 | 4.5 |
| 6 | 0.21 | 0.19 | 5 | 5 |

because the doping level is high, and therefore the permanent voltage and first harmonic amplitude voltage are smaller. Structure 6 has a maximum efficiency as the function of the current I_0 , but for

the optimum power point, this value is less than for structures 4 and 5. Besides, for this structure, it is necessary to increase the current value to 320 kA/cm^2 to obtain the optimum power point. Structures 5 and 6 have a maximum value of the real part of the total admittance, but have a greater doping level, and therefore a smaller value of the permanent and variable voltage and output power.

Semiconductor structures with a complex doping profile are analyzed for improving the power level and efficiency of the IMPATT diode with a maximum level of permanent current density. In Fig. 4 (a), (b) the dependencies of power level, efficiency and admittance are presented as functions of feeding current density I_0 for the optimum structure and for near optimum ones. Parameters of these structures are presented in Table 4.

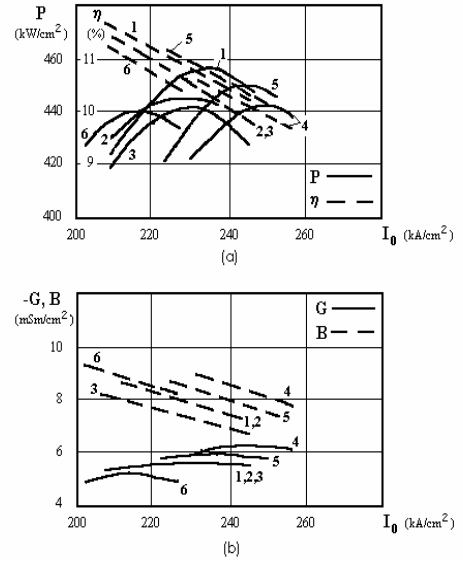


Figure 4. (a) Output power P and efficiency coefficient μ and (b) real G and imagine B parts of the total admittance as functions of feeding current density I_0 for optimal and near optimal structures with complex doping profile.

Table 4. Internal structure parameters for the diode with complex doping profile.

| n | $L1$ (10^{-4} cm) | $L2$ (10^{-4} cm) | $L3$ (10^{-4} cm) | $L4$ (10^{-4} cm) | $N1$ (10^{17} cm^{-3}) | $N2$ (10^{17} cm^{-3}) | $P2$ (10^{17} cm^{-3}) | $P1$ (10^{17} cm^{-3}) |
|-----|----------------------------------|----------------------------------|----------------------------------|----------------------------------|---------------------------------------|---------------------------------------|---------------------------------------|---------------------------------------|
| 1 | 0.09 | 0.08 | 0.11 | 0.06 | 1.6 | 4.7 | 4.1 | 1.6 |
| 2 | 0.09 | 0.08 | 0.11 | 0.06 | 1.5 | 4.7 | 4.7 | 1.5 |
| 3 | 0.09 | 0.08 | 0.11 | 0.06 | 1.6 | 4.7 | 4.1 | 1.4 |
| 4 | 0.09 | 0.08 | 0.11 | 0.06 | 1.6 | 5.2 | 4.6 | 1.6 |
| 5 | 0.08 | 0.09 | 0.12 | 0.05 | 1.6 | 4.7 | 4.1 | 1.6 |
| 6 | 0.07 | 0.08 | 0.11 | 0.04 | 1.6 | 4.7 | 4.1 | 1.6 |

Structure 1 is the optimal one. In this case, the power level is 457 kW/cm^2 , and the optimal current density value is 235 kA/cm^2 . Others structures are near this optimum one but have a lower power level and efficiency. The extension of the high doping level parts (structures 4 and 5) results in moving the power curve to a greater current density. These two types of semiconductor structures have a greater value of active admittance than the optimal one, but have a smaller microwave voltage and power level.

It is very important to compare the optimal characteristics for the two different types of structures as the constant doping profile (curve 4, Fig. 3(a)) and the complex doping profile (curve 1, Fig. 4(a)). A comparative analysis shows that the maximum output power level is quasi equal for two these optimal structures (436 kW/cm^2 and 452 kW/cm^2), but the efficiency coefficient has more difference (8.5% and 10.7%), quasi equal for two these optimal structures (436 kW/cm^2 and 452 kW/cm^2), but the efficiency coefficient has more difference (8.5% and 10.7%). The most important fact is a significant decrease of the optimal value of the permanent current density for the complex doping structure. For the permanent doping structure, the optimal current density value is 285 kA/cm^2 , but for the complex doping structure, it is 235 kA/cm^2 . Therefore, the complex doping profile structure has better energy characteristics, and allows the possibility to exploiting the diode under easier conditions.

5 Conclusions

Diode active layer optimization shows that the complex doping profile diode has a 6 % greater output power level and a 1.25-1.4 times greater efficiency coefficient with respect to the constant doping profile diode. The IMPATT diode with the complex doping profile has an appreciable gain with respect to the constant doping profile diode. This allows the possibility to obtain the maximum output power level with a smaller value of feed current density. The important feature of the optimal diode structure with a complex doping profile is a low sensitivity of the energy characteristics to the technological errors of the internal semiconductor structure. These complex semiconductor structures may be recommended for the increase of a real-time work period and the reliability of power pulsed-mode IMPATT diodes.

References:

[1] K. Chang, *Handbook of Microwave and Optical Components*, Vol. 1, John Wiley & Sons, New York, 1990.

- [2] A.M. Zemliak, and A.E. Roman, IMPATT Diode for the Pulsed-Mode, *Izvestiya VUZ Radioelectronika.*, Vol. 34, No. 10, 1991, pp.18-23.
- [3] M. Curow, Proposed GaAs IMPATT Devices Structure for D-band Applications, *Electron. Lett.* Vol.30, 1994, pp. 1629-1631.
- [4] M. Tschernitz, and J. Freyer, 140 GHz GaAs Double-Read IMPATT Diodes, *Electron. Lett.*, Vol. 31, No.7, 1995, pp. 582-583.
- [5] A. Zemliak, Models for Pulsed-Mode IMPATT Diode Simulation, *WSEAS Transactions on Systems*, Vol. 1, No. 2, 2002, pp. 222-231.
- [6] A.M. Zemliak, Difference Scheme Stability Analysis for IMPATT Diode Design, *Izvestiya VUZ Radioelectronika*, Vol.24, No.8, 1981, pp. 88-89.
- [7] H.J. Kafka, and K. Hess, A Carrier Temperature Model Simulation of a Double-Drift IMPATT Diode, *IEEE Trans. Electron Devices*, Vol.ED-28, 1981, pp. 831-834.
- [8] A.M. Zemliak, and S.A. Zinchenko, Non-linear Analysis of IMPATT Diodes, *Vestnik of the Kiev Polytech. Instit., Radiotechnika*, Vol.26, 1989, pp.10-14.
- [9] C. Dalle, and P.A. Rolland, Drift-Diffusion Versus Energy Model for Millimetric-Wave IMPATT Diodes Modelling, *Int. J. Numer. Modelling*, Vol.2, 1989, pp.61-73.
- [10] V. Stoiljkovic, M.J. Howes, and V. Postoyalko, Nonisothermal Drift-Diffusion Model of Avalanche Diodes, *J. Appl. Phys.*, Vol.72, 1992, pp. 5493-5495.
- [11] K.V. Vasilevskii, Calculation of the Dynamic Characteristics of a Silicon Carbide IMPATT Diode, *Sov. Phys. Semicond.*, Vol.26, 1992, pp. 994-999.
- [12] R.P. Joshi, S. Pathak, and J.A. Mcadoo, Hot-Electron and Thermal Effects on the Dynamic Characteristics of Single-Transit SiC Impact-Ionization Avalanche Transit-Time Diodes, *J. Appl. Phys.*, Vol.78, 1995, pp. 3492-3497.
- [13] O. Tornblad, U. Lindefelt, and B. Breitholtz, Heat Generation in Si Bipolar Power Devices: the Relative Importance of Various Contributions, *Solid State Electronics*, Vol.39, No.10, 1996, pp.1463-1471.
- [14] A. Zemliak, R. De La Cruz Jimenez, An Analysis of the Active Layer Optimization of High Power Pulsed IMPATT Diodes, *Computacion y Sistemas*, Edicion Especial, Dec. 2002, pp. 99-107.